polymer papers

Kinetic analysis of the crystallization of poly(*p*-phenylene sulphide)

Andrew J. Lovinger, D. D. Davis and F. J. Padden, Jr.
AT&T Bell Laboratories, Murray Hill, NJ 07974, USA
(Received 15 October 1984)

Growth rates of spherulites were measured in poly(*p*-phenylene sulphide) crystallized from the melt and the quenched glass over the temperature range 100°C–280°C, possibly the most extensive overall range yet reported for any polymer and, as such, most propitious for study of régime III crystallization. For a medium M.wt. polymer, a régime II → III transition was obtained at 208°C using values of transport parameters common to many polymers ($U^* = 1400$ cal mol^{-1}, $T_\infty - T_g = 30$°C) together with experimentally determined values of T_m^0 (315°C) and T_g(92°C). Under these conditions, the régime III/II slope ratio was found to be 2.07 (i.e. only 3.5% higher than predicted by régime theory), and reasonable estimates of surface free energies and of the work of chain folding were obtained. Other choices of the transport terms, including WLF and zero values, did not allow successful kinetic analyses. Although a régime I → II transition is predicted to occur at the high-temperature end of our growth-rate data, we found no experimental evidence for it. For a low M.wt. polymer, our analysis showed that régime III kinetics is obeyed at low temperatures, while at higher ones there is a continuous departure from that behaviour without, however, full attainment of régime II kinetics.

(Keywords: poly(*p*-phenylene sulphide); crystallization; growth rates; régime transitions; spherulites)

INTRODUCTION

Poly(*p*-phenylene sulphide), or PPS, is an important high-strength/high temperature polymer that is finding increasing use in contemporary technological applications, such as connectors for electrical and optical-fibre cables, chip carriers, printed-wiring board substrates, and electronic-component encapsulants[1–3]. In addition, it has recently generated much interest as being the first melt- and solution-processable polymer that can be rendered electrically conductive[4,5]. Since these desirable macroscopic properties are directly related to the structure and processing history of each particular sample, we have recently embarked upon a detailed study of the crystallization and morphology of PPS. This work has been concerned with the growth of single crystals and polycrystalline aggregates from solution[6], the determination of morphological characteristics of melt-grown samples (including unique thin-film morphologies)[7], and the examination of structural and morphological changes accompanying doping with conductivity-enhancing materials[8].

As part of our study, we have also investigated the crystallization kinetics of PPS, which are reported here. We have found this polymer to be an ideal candidate for analysis of kinetic data because we could crystallize it isothermally over an exceptionally wide temperature range that approaches both the glass- and the melting transitions. This wide range of crystallization temperature is of primary importance for a reliable analysis of growth-rate data based on the established kinetic nucleation theory of Hoffman and co-workers[9,10], and particularly for its recent extensions to low temperatures (régime III)[11]. The theory predicting existence of such a régime[11], while supported by limited data from a few polymers, is still awaiting experimental confirmation from polymers that can be crystallized over broad temperature ranges. As discussed in detail in the following section of this report, régime III behaviour has been inferred to date from measurements on four polymers (polyethylene[11,12], isotactic polypropylene[13], poly(oxymethylene)[11,14] and *cis*-1,4-polyisoprene[15]) spanning only narrow ranges of crystallization temperature (i.e. less than about 40°C)*. On the other hand, polymers such as isotactic polystyrene[16–18], nylon-6[19,20] and poly(tetramethyl-*p*-silphenylene siloxane)[21,22] that have been examined over much wider domains of crystallization temperature (*ca.* 100°C) have exhibited no régime breaks in the growth-rate curves[9,23]. As we show in this paper, PPS of sufficiently high molecular weight, crystallized within a very extensive temperature interval (> 160°C) displays an unequivocal régime transition and offers the broadest experimental confirmation of régime III.

BACKGROUND

The radial growth rates of polymeric spherulites are the same as those of their constituent lamellar crystals[24,25], and may be expressed as functions of undercooling from their equilibrium melting points according to the well-known equation of Hoffman *et al.*[9,10]

$$G = G_0 \exp[-U^*/R(T_c - T_\infty)] \exp[-K_g/T_c(\Delta T)f]. \quad (1)$$

Here, G_0 is a pre-exponential factor that includes all terms that are taken as effectively independent of temperature. The first exponential contains the contribution of diffusional processes to the growth rate and is closely analogous to the segmental jump rate encountered in

* Since submission of our manuscript, a régime II → III transition has also been found in a biological polymer (poly-3-hydroxybutyrate) crystallized between ~45°C and 160°C (Barham, P. J., Keller, A., Otun, E. L. and Holmes, P. A. *J. Mater. Sci.* 1984, **19**, 2781)

0032-3861/85/111595-10$03.00

viscoelastic analyses[26,27]. U^* is the activation energy for chain motion, T_∞ the temperature below which such motion stops, T_c the crystallization temperature, and R the gas constant. The first two of these are taken from the WLF equation where $U^* = 4120$ cal mol^{-1} and $T_\infty = T_g - 51.6$ K (T_g is the glass transition temperature). While these values are generally associated with viscoelastic measurements, they are less applicable to crystallization rate analyses; for most polymers, values of U^* in the vicinity of 1500 cal mol^{-1} and $T_\infty = T_g - 30$ K are optimal[9]. The second exponential in equation (1) is a strong function of crystallization temperature T_c, and undercooling ΔT, where $\Delta T (\equiv T_m^0 - T_c)$ is measured from the thermodynamic melting point T_m^0 of samples with the same molecular characteristics (i.e. molecular weight and polydispersity) as those used in the growth rate study. The factor f is a correction term that is close to unity at high temperatures, but that becomes of importance at high undercoolings where the heat of fusion varies significantly with temperature; it is given empirically as[9]

$$f = 2T_c/(T_m^0 + T_c). \quad (2)$$

The term K_g is important in that it contains the variable n that reflects the régime behaviour. Specifically,

$$K_g = nb_0\sigma\sigma_e T_m^0/(\Delta h_f)k \quad (3)$$

where n is a constant that equals 4 for régimes I and III, and 2 for régime II, b_0 is the molecular thickness, σ is the lateral-surface free energy, σ_e the end-surface free energy, Δh_f the enthalpy of fusion, and k Boltzmann's constant.

Régime behaviour, described in detail in Hoffman's recent work[9,11], is determined by the mechanism of growth of molecular layers adsorbed on the exposed surface of a lamellar crystal. Briefly, at the highest temperatures, the rate of molecular nucleation is sufficiently small that adsorbed molecules can freely spread by chain-folding along the width of the lamellar substrate before a new nucleation event occurs. This temperature region is defined as régime I, for which the overall growth rate is proportional to the rate of molecular nucleation, and n equals 4 in equation (3). Similarly, at low temperatures (high undercoolings), overall growth is again directly proportional to the rate of nucleation, because the latter is now so high that adsorbed molecular stems have little, if any, room to spread laterally; crystallization proceeds almost exclusively through accumulating nucleation events, leading to high kinetic roughness at growth fronts. Under these conditions (régime III) n is again equal to 4. Finally, at intermediate temperatures, the growth behaviour is also intermediate between régimes I and III: nucleation now occurs at higher rates than in régime I, so that adjacent nuclei must compete in spreading laterally on the crystal substrate; at the same time, nucleation is not so dense as in régime III to hinder such lateral growth. In this régime II, the overall crystal growth rate is proportional to the square root of the nucleation rate, with the result that n is now equal to 2.

The typical shape of experimentally determined growth-rate *versus* temperature curves is seen schematically in *Figure 1a*, where the first and second exponentials of equation (1) are responsible for the decays in G at low and high temperatures, respectively. However, according to régime theory[9-11], these curves should exhibit breaks corresponding to régime I → II and II → III transitions, as depicted in the same Figure. The location of these transitions may be established by the usual kinetic analysis, which involves plotting equation (1) in logarithmic form as $\log G + U^*/[2.303R(T_c - T_\infty)]$ *versus* $1/[T_c(\Delta T)f]$. As seen in *Figure 1b*, such a plot should, in the most general case, consist of three straight-line segments that correspond to the three régimes of crystallization. Each segment would then yield a slope and intercept proportional to K_g and G_0, respectively, with slopes changing by a factor of 2 at the régime transitions. In actual practice, the situation has so far been much less clear, with most polymers following a single straight-line behaviour, and with only very few exhibiting discernible régime I → II or II → III transitions.

In an attempt toward understanding the reasons for this discrepancy, we have plotted in *Figure 2* the published growth-rate data for a great number of polymers, as identified in the accompanying *Table 1*. While this compilation is certainly not exhaustive, it gives a clear composite picture of the extent of crystallization data available for polymers. The growth rate curves in *Figure 2* have been shifted vertically in order to prevent gross overlaps; the extent of an order-of-magnitude change in growth rate is marked in this figure. The most obvious and important conclusion to be drawn from these curves is that crystallization data could be obtained for most polymers over only very limited regions of their full growth-rate curves. These regions generally tend to be concentrated toward high temperatures, where régime

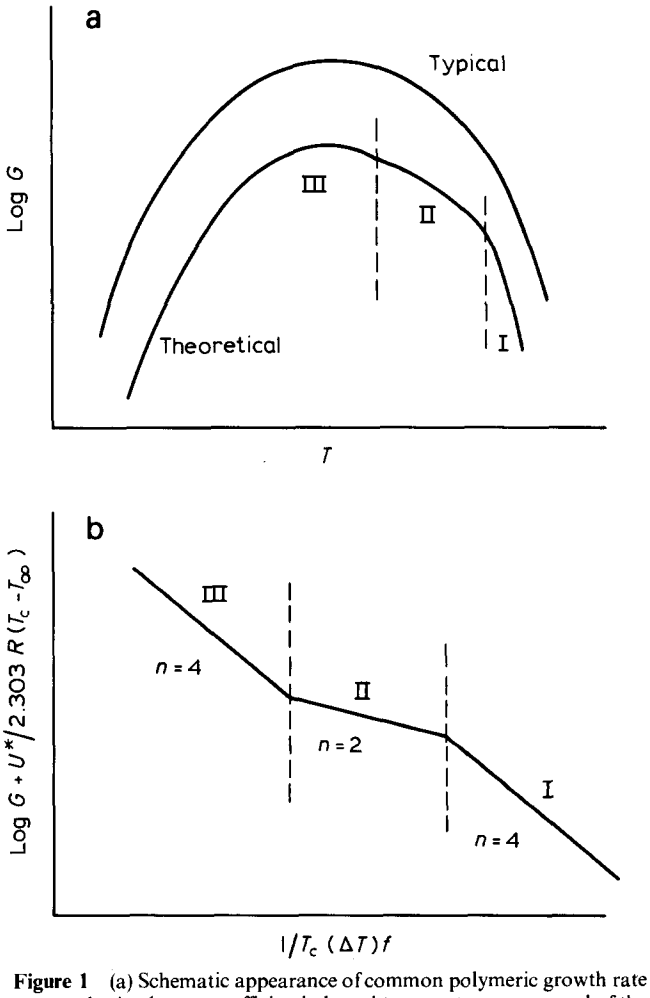

Figure 1 (a) Schematic appearance of common polymeric growth rate curves obtained over a sufficiently broad temperature range, and of the theoretical shape showing régime behaviour. (b) Kinetic analysis of illustrative growth rate curve showing régime transitions

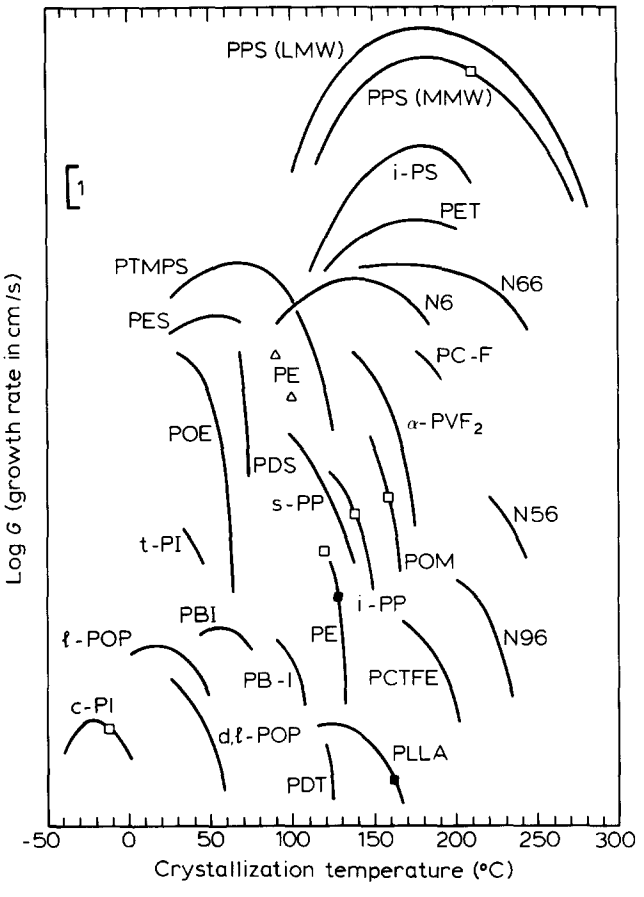

Figure 2 Growth rate curves for a number of polymers (identified in *Table 1*) showing the extent in temperature and in log G for each. The curves are arbitrarily shifted along the ordinate to remove overlaps. The scale bar represents one unit in log G. (■) régime I → II transitions; (□) régime II → III transitions; (△) low-temperature polyethylene growth data[12]

Table 1 Compilation of polymer growth rate data for *Figure 1*

Abbreviation	Polymer	Refs.
N6	Nylon-6	19, 20
N56	Nylon-5,6	28
N66	Nylon-6,6	29
N96	Nylon-9,6	28
PBI	Poly(butylene isophthalate)	30
PB-1	Poly(butene-1), Form II	31
PC-F	Polycarbonate-F	32
PCTFE	Polychlorotrifluoroethylene	33
PDS	Poly(decamethylene sebacate)	34
PDT	Poly(decamethylene terephthalate)	35
PE	Polyethylene	9, 12, 36, 37
PES	Poly(ethylene succinate)	38
PET	Poly(ethylene terephthalate)	39
c-PI	*cis*-1,4-Polyisoprene (α-phase)	15,40
t-PI	*trans*-1,4-Polyisoprene (β-phase)	41
PLLA	Poly(L-lactic acid)	42
POE	Poly(oxyethylene)	24, 25
POM	Poly(oxymethylene)	14
d,l-POP	*d,l*-Poly(oxypropylene)	43
l-POP	*l*-Poly(oxypropylene)	43
i-PP	Isotactic polypropylene (α-phase)	13, 44–46
s-PP	Syndiotactic polypropylene	47
PPS (LMW)	Poly(*p*-phenylene sulphide), low M.wt.	This work
PPS (MMW)	Poly(*p*-phenylene sulphide), medium M.wt.	This work
i-PS	Isotactic polystyrene	16–18
PTMPS	Poly(tetramethyl-*p*-silphenylene siloxane)	21, 22
α-PVF_2	Poly(vinylidene fluoride), α-phase	23, 48, 49

II → III transitions are very unlikely to be located; régime I → II transitions might be observable in this range, but only if sufficiently small undercoolings are attained. The latter has been the case in polyethylene and poly(L-lactic acid), which to our knowledge are the only polymers for which régime I → II transitions have been reported. On the other hand, it is surprising that polymers such as poly(oxyethylene), poly(tetramethyl-*p*-silphenylene siloxane), and poly(vinylidene fluoride), with extensive ranges of log G at high temperatures could be successfully analysed using single straight-line plots and without discernible régime I → II breaks.

In regard to régime II → III transitions, they have been postulated by Hoffman for polyethylene[11] (with experimental corroboration from two low-temperature growth estimates by Martinez-Salazar *et al.*[12]), and have also been demonstrated by him in isotactic polypropylene[13] and poly(oxymethylene)[11]. The latter case is remarkable in that the régime II → III transition is accompanied by major morphological changes (from hedritic to spherulitic)[14] that are more consistent with a régime I → II transition. It is, in fact, not yet clear what morphological changes, if any, might be expected at régime II → III transitions; in addition to the atypical behaviour of poly(oxymethylene), there are changes in birefringence for isotactic polypropylene in the region of this transition, but these are complicated by the uniquely branched lamellar microstructure of this polymer. A régime II → III transition has also recently been proposed for *cis*-1,4-polyisoprene[15], but only for an uncommon choice of U^* and T_∞, and with a significant departure of the slope ratio from the expected value of 2. This paucity of confirmed régime II → III transitions is somewhat surprising, particularly if we note from *Figure 2* that for a few polymers (i.e. isotactic polystyrene, nylon-6, poly(ethylene terephthalate), and poly(tetramethyl-*p*-silphenylene siloxane)) growth-rate data exist that extend well within the region of diffusion-controlled crystal growth*.

Consideration of the growth rate curves for PPS (as determined in this study) at the top of *Figure 2*, and comparison with growth rate data for other polymers, demonstrates that this polymer is exceptionally amenable to régime analysis. The temperature scale over which growth-rate measurements could be obtained for PPS is the widest among all polymers in *Figure 2* and extends highly both above and below the temperature of the peak rate. Our detailed investigation of the growth kinetics of PPS is presented below.

EXPERIMENTAL

Two samples of PPS, prepared by condensation polymerization and manufactured by Phillips Petroleum Company, were employed in our studies. The first was a commercial sample, Ryton® V-1, of low molecular weight ($\bar{M}_w \sim 15\,000$)[50]. The second was a research-grade, medium-molecular-weight sample ($\bar{M}_w \sim 51\,000$)[50], kindly donated by Dr T. W. Johnson of Phillips Petroleum Co. Both had polydispersities in the range of 1.3–1.7 (ref. 50).

The PPS specimens were moulded into very thin films between glass cover slips for spherulitic growth rate measurements in a Mettler FP51 microscope heating

* For an additional newly discovered régime II → III transition see preceding footnote

stage that had been calibrated using melting-point standards. We found the nucleation density of PPS to be very high, even in specimens from which traces of ionic by-products of the polymerization reaction[51,52] had been removed by water extraction. For this reason, it was important to prepare films as thin as possible. A major technique for reducing nucleation density in a crystallizing polymer involves use of high temperatures and long durations of superheating in the melt. This could be used only to a very limited extent, because PPS is known to undergo chemical reactions at high temperature that alter its molecular characteristics; these reactions involve primarily chain extension and crosslinking[53,54]. For this reason, the samples were held at 330°C (M.pt. ~290°C) for only 30 s prior to isothermal crystallization under dried nitrogen. This treatment was effective in reducing nucleation density to the point of allowing spherulitic growth rate measurements.

Crystallizations from the melt were conducted between 200°C and 280°C, and over the minimal possible residence times, again so as to prevent significant molecular changes at high temperatures. Residence times did not exceed 2 h and were always well below the point of departure from linearity of the increase in spherulitic diameter. To attain such relatively short residence times at the highest temperatures, spherulites were first rapidly nucleated at lower temperatures. Cyrstallizations of specimens warmed from the glassy state were performed between 100°C and 220°C; these specimens had originally been quenched from the melt to ambient or liquid-nitrogen temperatures. No significant variation of growth rates was noted for samples differing in quench temperature, or for those that were crystallized at the same temperature from either the cooled melt or from the warmed glass.

Growth rate measurements were always conducted on freshly made films. In each specimen, growth rates were determined for numerous spherulites (range 3–11, depending upon nucleation density) by plotting their diameters (measured in various directions from optical micrographs) as functions of time, and then calculating the slopes of the best straight lines. At almost all temperatures, duplicate or multiple samples were again examined in the same manner, so that the growth rates reported here represent reliable averages, as discussed by Miller[23].

For determination of the thermodynamic melting point corresponding to each molecular weight, samples encapsulated in aluminium pans were isothermally crystallized for 1 h at selected temperatures (after being held at 330°C for 30 s) and then heated through their melting transition in a computer controlled DuPont 1090 Thermal Analyzer at a rate of 5°C/min. Glass transition temperatures for the LMW and MMW samples were determined as 84°C and 92°C, respectively, in a Perkin Elmer DSC-2 calorimeter at a heating rate of 20°C/min. For both T_m and T_g measurements, the calorimeters had been calibrated at the corresponding rates using melting point standards.

RESULTS

Thermodynamic melting points

Both the low- and the medium-molecular weight samples exhibited a melting behaviour at all temperatures that indicates presence of only one crystalline phase. As is shown in a separate morphological study[7], the crystallographic characteristics of this phase are consistent with the unit cell of Tabor *et al*[55], in which the sulphur atoms define a planar zigzag with a repeat of 10.26 Å, and the phenylene rings are inclined alternately by $\pm 45°$ to the plane of that zigzag. Construction of Hoffman–Weeks plots from our d.s.c. data yields extrapolated melting points of 303°C and 315°C for our two PPS samples (see *Figure 3*).

Growth analysis of LMW PPS

Growth rate curves for both the low- and medium-molecular weight samples of PPS, determined as described in the Experimental section, are presented in *Figure 4*. The first of these has a maximal growth rate around 180°C, while the second shows a broader plateau.

We have analysed the data from the LMW polymer with the aid of equations (1) and (2), as seen in *Figure 5*. Here, the experimentally determined values of T_m^0 and T_g were used, and T_∞ was taken as $T_g - 30$ K, in common with most other polymers[9]. It is clear from *Figure 5a*, which covers the full 180°C range of crystallization

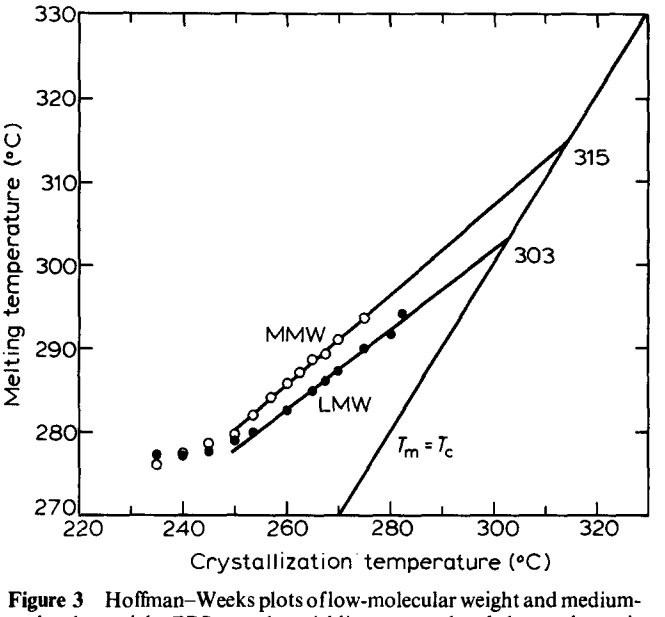

Figure 3 Hoffman–Weeks plots of low-molecular weight and medium-molecular weight PPS samples, yielding extrapolated thermodynamic melting points

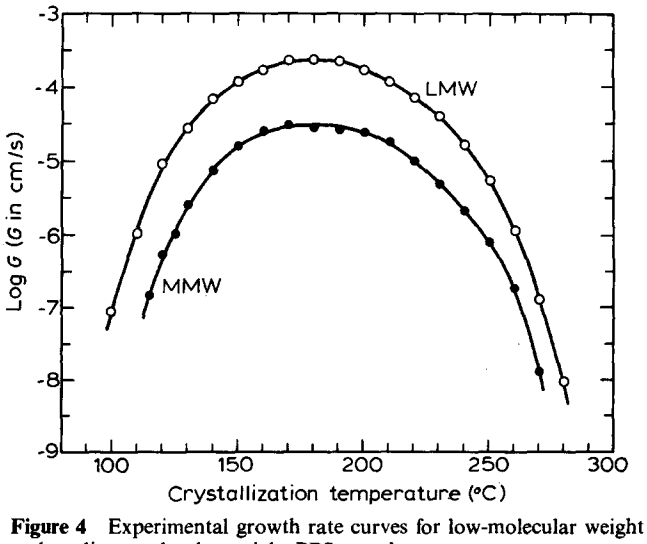

Figure 4 Experimental growth rate curves for low-molecular weight and medium-molecular weight PPS samples

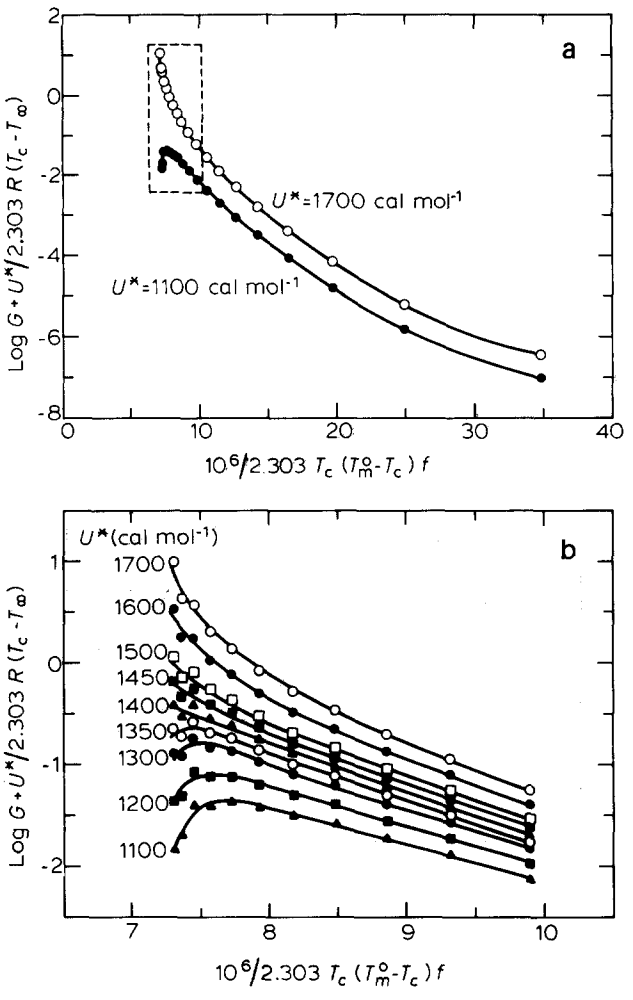

Figure 5 (a) Kinetic analysis of the growth rate data for LMW PPS using two different values of U^*. (b) Enlargement of the low-temperature region of *a* and incorporation of curves for intermediate values of U^*. $T_m^0 = 303°C$, $T_g = 84°C$, $T_\infty = T_g - 30°C$

temperatures, that the data cannot be linearized with one or more straight lines: for a selected value of $U^* = 1700$ cal mol^{-1}, the curve has a continuous positive curvature throughout, while for $U^* = 1100$ cal mol^{-1}, it shows an inflection at low temperatures. Because of this sensitivity of the curvature to U^*, we attempted to linearize the low-temperature data by selecting an appropriate intermediate value of the activation energy, as seen in *Figure 5b*. The best linear fit is obtained for $U^* = 1400$ cal mol^{-1} (correlation coefficient = 0.9959). When this line is superimposed on our full set of data (*Figure 6*), it is seen that at high temperatures there are large deviations from the calculated behaviour. Moreover, these cannot be compensated by invoking a discrete régime transition, because no second straight line can be drawn through the high-temperature points, as they exhibit a pronounced and systematic positive curvature. In fact, the only manner by which an approximate straight-line behaviour may be forced, is to increase substantially the value of T_m^0. As seen in *Figure 6*, arbitrary selection of an exceptionally high T_m^0 (330°C) suppressed the curvature to the point of allowing a straight line to be drawn for $U^* = 1275$ cal mol^{-1}. That this is an experimentally unacceptable analysis of our results is inferred not only from the systematic (rather than statistical) deviation of the data points in *Figure 6* from this straight line, but, more clearly, from a second look at *Figure 3*, which shows 330°C to be a totally unrealistic value for the T_m^0 of this LMW PPS.

Since the transport values common to many polymers (i.e. $T_\infty = T_g - 30$ K, and U^* in the vicinity of 1500 cal mol^{-1})[9] do not result in a successful kinetic analysis for this LWM PPS, we have examined how WLF transport values affect this analysis. A case where the latter (i.e. $U^* = 4120$ cal mol^{-1} and $T_\infty = T_g - 51.6$ K) yielded a more successful kinetic analysis of the growth rate data is that of *cis*-1,4-polyisoprene (α-phase)[15]. Nevertheless, for our LMW PPS this is not so, as may be seen in *Figure 7*. At low temperatures, the curve drops sharply for low values of U^* but increases rapidly for $U^* > \sim 2800$ cal mol^{-1} (i.e. well below the WLF value). In addition, because of the high curvature, even the low-temperature linearization is less successful than for the case of $T_\infty = T_g - 30$ K (*Figure 6*). At the same time, the problem of the pronounced positive curvature at high temperatures still persists.

Changing the value of T_∞ in the opposite direction (i.e. toward T_g) does not improve the analysis, either. For example, using $T_\infty = T_g - 10$ K allows linearization of fewer low-temperature data than for $T_g - 30$ K, with a poorer correlation coefficient, and with a very low value of U^* (680 cal mol^{-1}). This lack of improvement with different manipulations of U^* and T_∞ is not surprising, because these parameters affect significantly only the low-temperature part of the growth rate curve, but are of very little influence at high temperatures where the dominant log G term shows a pronounced positive curvature.

We can now complete this kinetic analysis of LMW PPS by showing in *Figure 8* the best calculated growth-rate *versus* temperature curves superimposed on our data. For the experimentally obtained T_m^0 of 303°C, good

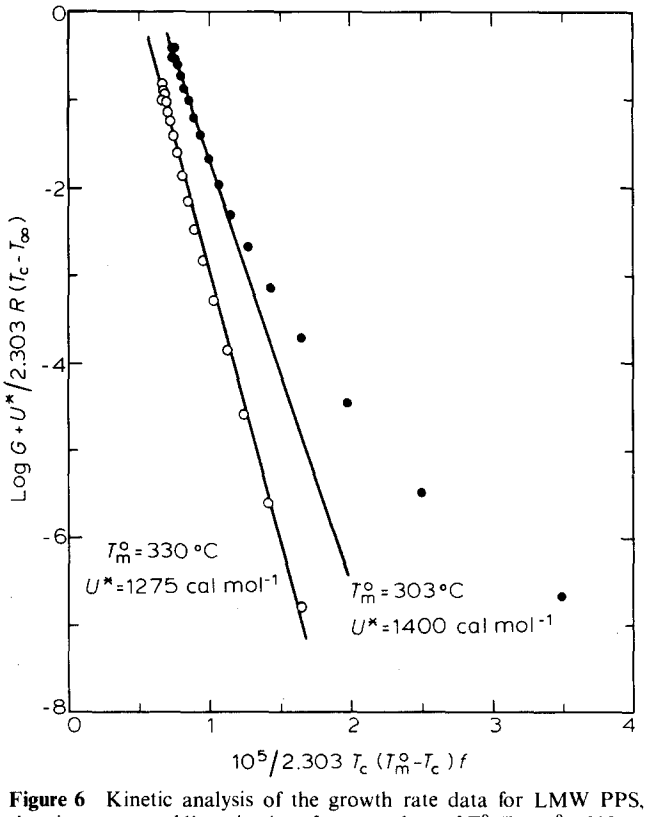

Figure 6 Kinetic analysis of the growth rate data for LMW PPS, showing attempted linearizations for two values of T_m^0. For $T_m^0 = 303$°C, the low-temperature data have been fitted to a straight line, while for $T_m^0 = 330$°C, all data have been so fitted

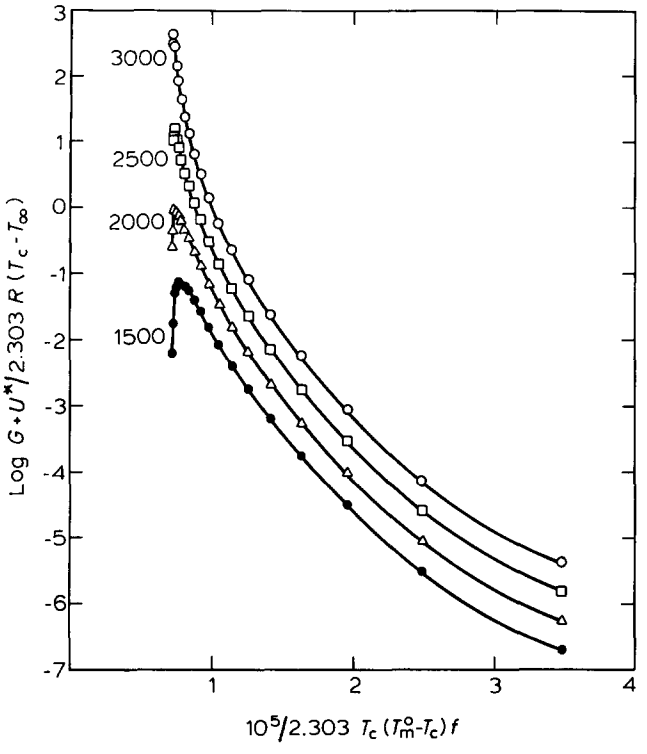

Figure 7 Kinetic analysis of the growth rate data for LMW PPS, using different values of U^* (cal mol^{-1}). $T_m^0 = 303°C$, $T_g = 84°C$, $T_\infty = T_g - 51.6°C$

agreement is seen up to 200°C, with deviations increasing thereafter. Better agreement over the full temperature range (although still with systematic deviations) is obtained only for unrealistically high values of T_m^0 (330°C). We therefore conclude that this low-molecular weight PPS sample cannot be successfully analysed over the full range of crystallization temperatures. Linearization at low temperatures (as seen in *Figures 5* and *6*) implies régime III behaviour, whereas the continuous positive curvature at higher temperatures shows deviations from that régime, albeit without full adoption of régime II kinetics. Possible reasons for these growth characteristics of LMW PPS are analysed in the Discussion.

Growth analysis of MMW PPS

Growth rate data for the medium-molecular weight polymer (seen in *Figure 4*) were analysed as above to test their régime behaviour and overall conformity with the kinetic theory of crystallization. For the sake of brevity, we present our results in combined form for two values of T_∞ corresponding to 30 K and 51.6 K below T_g. The low-temperature region of curves obtained by plotting equation (1) in logarithmic form is depicted in *Figure 9*. For both choices of T_∞, the curves are seen at the lowest temperatures to diverge upwards with increasing U^* and downwards with decreasing U^*. As before, there exists an intermediate value of U^* for each T_∞ that permits optimal linearization of the data within this temperature range. For $T_\infty = T_g - 30$ K, this value of U^* is 1400 cal mol^{-1} (correlation coefficient = 0.9968), while for $T_\infty = T_g - 51.6$ K, the corresponding U^* equals 2650 cal mol^{-1} (correlation coefficient = 0.9976). We should note that the value of 1400 for U^* is identical to the one found for the LMW PPS at the same T_∞ ($= T_g - 30$ K), and is also well within the range of 1300 ± 300 cal mol^{-1} shown to be typical of most polymers[9,23]. On the other hand, just as in the case of LMW PPS, here, too, the choice of $T_\infty = T_g - 51.6$ K does not allow us even to approach the corresponding WLF value for U^*, i.e. 4120 cal mol^{-1}.

If we now apply these values of the transport coefficients U^* and T_∞ to our *full* set of growth rate data (see *Figure 10*), a remarkable difference from the behaviour of LMW PPS becomes apparent: the high-temperature data do not exhibit any systematic curvature, but fall instead neatly on straight lines with very high correlation coef-

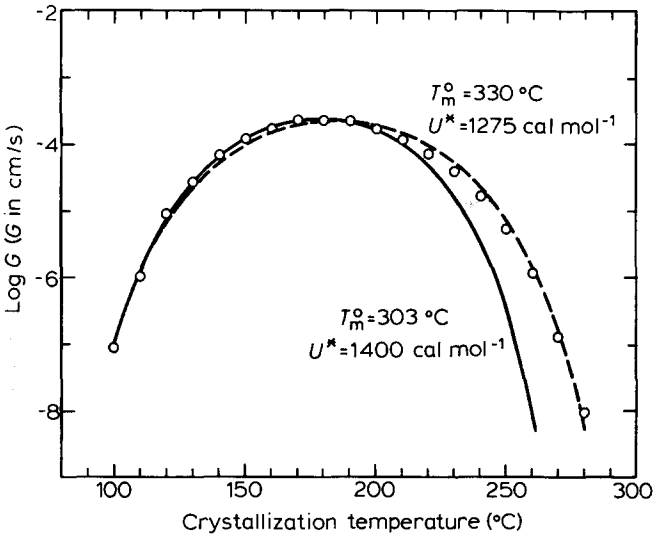

Figure 8 Calculated growth rate curves using two different sets of values for T_m^0 and U^*, superimposed upon the experimental data for LMW PPS

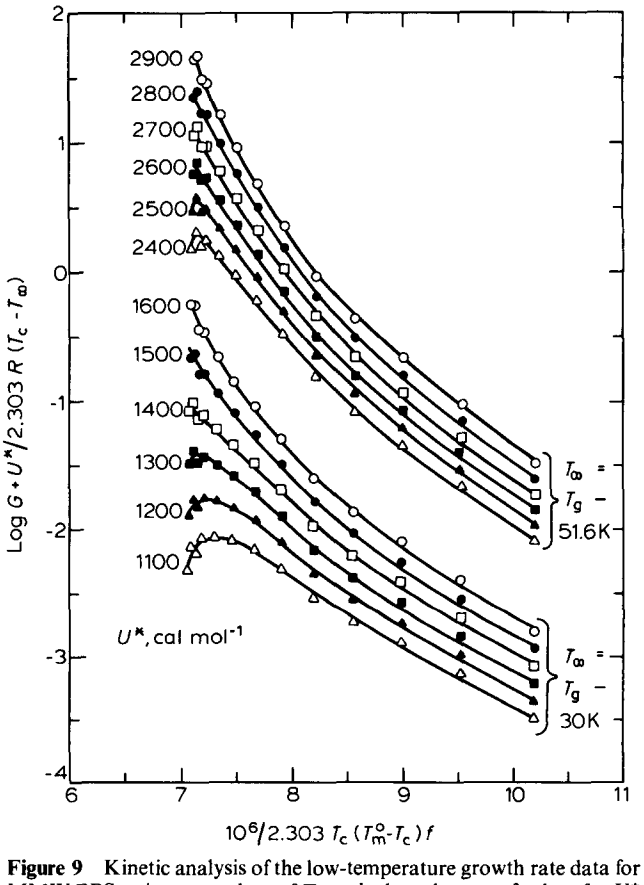

Figure 9 Kinetic analysis of the low-temperature growth rate data for MMW PPS, using two values of T_∞ and a broad range of values for U^* (cal mol^{-1}). $T_m^0 = 315°C$, $T_g = 92°C$

ficients (see *Table 2*). This table also contains the slopes and intercepts of these lines, which appear clearly to support a distinct régime behaviour, particularly for the case of $T_\infty = T_g - 30$ K for which the slope ratio is found to be 2.07 (i.e. only 3.5% higher than predicted[11]). Although two well-defined linear regions are also obtained for the case of $T_\infty = T_g - 51.6$ K, not only is the corresponding value of U^* inappropriately low, but the slope ratio for these lines (i.e. 3.03) is much too high in regard to the predicted value for a régime III → II transition. We should also note from *Figure 10* that there are three intermediate data points that do not lie on either of the régime lines but provide a smooth bridge between them; we attribute the lack of a sharp break to polydispersity, branching, and other molecular defects in these commercial samples.

Based on this analysis, we can now superimpose these calculated curves on our growth rate data. *Figure 11*

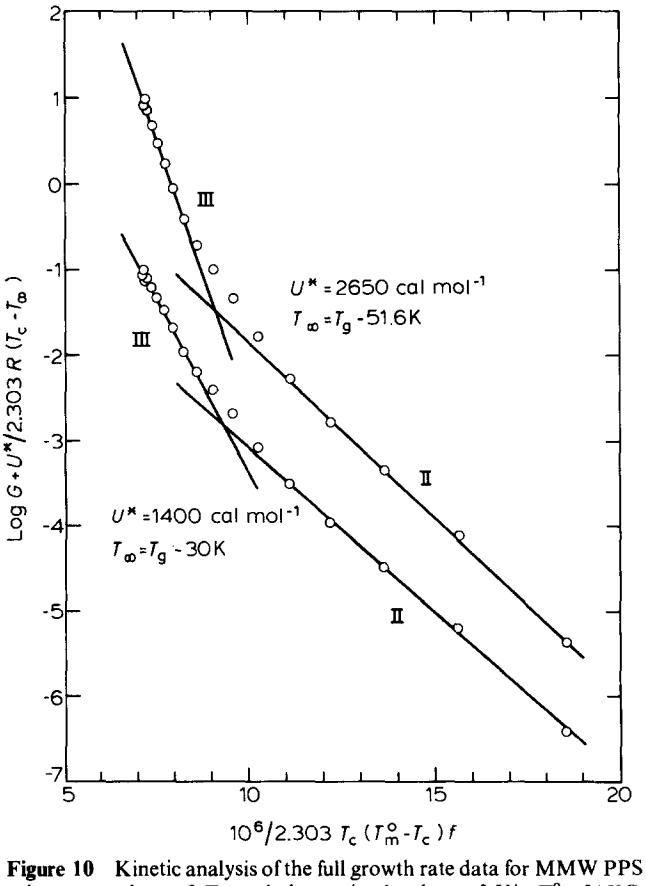

Figure 10 Kinetic analysis of the full growth rate data for MMW PPS using two values of T_∞ and the optimal values of U^*. $T_m^0 = 315$°C, $T_g = 92$°C

Table 2 Values of kinetic parameters for MMW PPS determined from *Figure 10*

	$T_\infty = T_g - 30$ K		$T_\infty = T_g - 51.6$ K	
U^* (cal mol^{-1})	1400		2650	
	Rég. II	Rég. III	Rég. II	Rég. III
Slope × 10^{-5} (K^2)	−3.841	−7.970	−4.076	−12.340
$K_g \times 10^{-5}$ (K^2)	8.84	18.35	9.39	28.42
Correlation coefficient	0.9994	0.9968	0.9996	0.9976
G_0 (cm/s)	5.43	3.86×10^4	1.61×10^2	4.67×10^9
K_g^{III}/K_g^{II}	2.07		3.03	

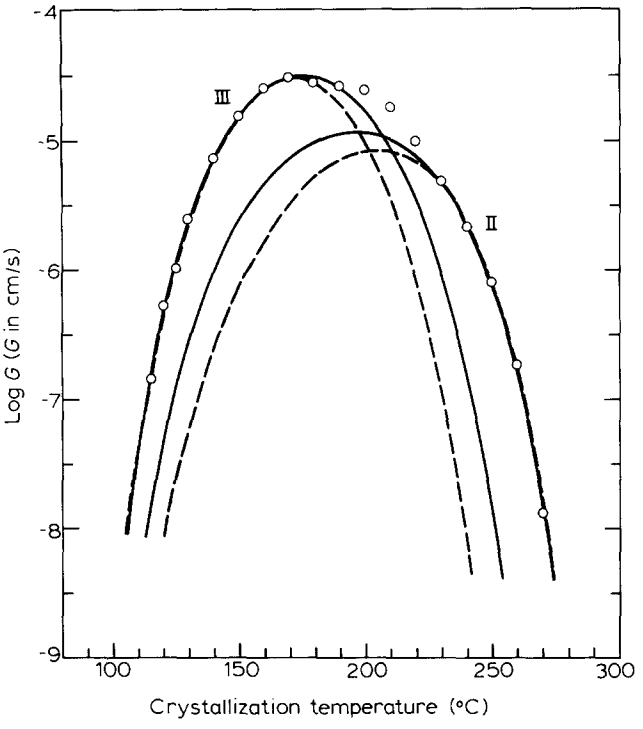

Figure 11 Calculated growth rate curves using two different sets of values for T_∞ and U^*, superimposed upon the experimental growth data for MMW PPS. Solid line: $T_\infty = T_g - 30$ K, $U^* = 1400$ cal mol^{-1}; broken line: $T_\infty = T_g - 51.6$ K, $U^* = 2650$ cal mol^{-1}

shows such superposition for both sets of T_∞ and U^* values. The much better correspondence of the curves for $U^* = 1400$ cal mol^{-1} with our experimental data is clearly evident. From all of the above, we conclude that the medium M.wt. PPS, in contrast to its low M.wt. counterpart, behaves consistently with régime behaviour over the full growth temperature range, and shows a régime III → II break at 208°C for values of transport coefficients that are well within the range typical of most other polymers.

DISCUSSION

Régime II → III transition

Our results on medium M.wt. PPS offer the most extensive agreement yet with régime III predictions. Because a large proportion of our growth rate data falls within the region of diffusion-controlled growth, they provide a most sensitive test of the applicability of various transport parameters. As we have shown above, we have found the WLF values inapplicable to the kinetic analysis of this polymer, and the values suggested by Hoffman[9] in excellent agreement with our experimental results. Although (for the sake of brevity) we have not included an additional set of curves for the case $T_\infty = T_g$, we have examined it, since for a number of polymers (e.g. PVF_2, POE) this choice of transport term provides a fit at least as good as[23] the choice of $T_\infty = T_g - 30$ K. In contrast to these polymers, where the analysis is fairly insensitive to the choice of viscosity parameters, MMW PPS showed a much poorer correlation for values of T_∞ other than $T_g - 30$ K, and, in fact, did not allow linearization at low temperatures for the case of $T_\infty = T_g$.

We should also enquire at this stage as to why our low M.wt. PPS cannot be analysed successfully with any selection of constants, but displays instead a continuously

positive curvature. The reason for this may be associated with the very limited number of adjacent stems that are possible for this LMW polymer. As shown in our morphological study[7], the thickness of melt-grown PPS crystals was determined by electron microscopy as 12–20 nm. Using the unit-cell structure of Tabor *et al.*[55], we then find that a 15 000$\bar{M}_w$ chain culd provide only 3–6 adjacent stems in such crystals. We do not expect this to be adequate for a well-defined régime-II behaviour, because the number of stems barely exceeds the mean niche separation for régime III (2–4 stems)[11], so that the effects of chain ends in introducing disorder will be proportionately very high. This is expected to be particularly true for PPS because of its stiff chains and because of the different chemical moieties at the chain ends of this condensation polymer. Therefore, as we found experimentally, régime III behaviour should be followed exactly at low temperatures (as shown by the successful linearization in *Figure 6*), while at higher ones a gradual departure could be expected, without, however, full attainment of régime II kinetics. In contrast, the medium M.wt. polymer ($\bar{M}_w \sim 51\,000$) allows formation of 12–21 adjacent stems within the aforementioned crystal thickness; here, the effects of chain ends on substrate completion are proportionately reduced, so that full adoption of régime II kinetics should be much more likely.

The régime II → III transition found here for MMW PPS did not appear to be accompanied by any significant morphological changes (this is discussed more fully in our paper on morphology of PPS[7]). On the basis of the molecular-attachment processes characterizing these two régimes, we would expect only small morphological changes at their transition (especially in comparison with the régime I → II transition, which for polyethylene involves an axialitic → spherulitic modification). In this context, the gross hedritic → spherulitic changes accompanying the régime II → III transition in polyoxymethylene are surprising and may be exceptional.

A final question relative to the régime II → III transition in PPS is why have similar transitions been found in only so few other polymers. As we have seen from *Figure 2*, growth-rate data for most polymers do not extend to temperatures low enough to allow clear adoption of régime III kinetics. A few, however, such as PTMPS, nylon-6, poly(ethylene terephthalate), and isotactic polystyrene, *do* encompass sufficiently low temperaturres to enter régime III. Although the crystallization of these polymers had been analysed before the advent of régime III, it is still puzzling that deviations from régime II behaviour were not noted, particularly for isotactic polystyrene, for which the great majority of growth-rate data originates from temperatures that should be well within régime III (see again *Figure 2*). In view of the increasing experimental evidence for régime III, re-examination of the growth kinetics of these polymers might be fruitful.

Estimates of thermodynamic parameters

The values of the slopes and intercepts of the régime II and III lines from *Figure 10* and *Table 2* can be used to estimate corresponding values of the surface free energies and of the work of chain folding for PPS. The lateral surface free energy, σ, may be estimated from[9]

$$\sigma = \alpha \Delta h_f A^{1/2} \qquad (4)$$

where α is a constant ranging from 0.1 to 0.3 and A is the molecular cross-sectional area. For (020) growth planes, the molecular width (a_0) is 4.33 Å and the molecular thickness (b_0) is 5.6 Å, so that $A = 24.30$ Å^2. The heat of fusion of the fully crystalline polymer is not known. Nevertheless, we shall use the results of Brady[51], who obtained a $\Delta h_f \simeq 12$ cal/g for a PPS sample of ~63% crystallinity, to extrapolate to a value of ~19 cal/g (or ~80 J/g) for the heat of fusion of the 100% crystalline material. The value of α is close to 0.1 for polyolefins[9], but for other organic molecules it is closer to 0.3 (ref. 57). By choosing these two limiting values of α, we obtain the estimates for σ given in *Table 3*. The choice of $\alpha = 0.3$ gives a value for the lateral surface free energy that is very close to those from other polymers[9,11,13], whereas the value for σ using $\alpha = 0.1$ appears too low.

Calculation of the end- or fold-surface free energy, σ_e, is based on equation (3) using the above values for σ, b_0, and Δh_f and the appropriate values for K_g and n for régimes II and III. Our resulting estimates for σ_e are seen again in *Table 3*. As expected, there is good agreement between the régime II and III estimates for both choices of α. Here, too, the selection of $\alpha = 0.3$ yields values of σ_e in close correspondence with those for other polymers[9,11,13]; σ_e values appear unreasonably high for $\alpha = 0.1$.

The work of chain folding is obtained directly from the end-surface free energy, as[9]

$$q = 2\sigma_e A. \qquad (5)$$

Values of q given in *Table 3* once again suggest that α should be taken nearer to 0.3 than to 0.1. This is because q has been found[9] to be the parameter most closely correlated with molecular structure: very flexible chains (such as in polyethers) have values around 3 kcal mol^{-1}, intermediate ones (e.g. polyethylene) around 5 kcal mol^{-1}, while stiff ones (such as polystyrene or polytetrafluoroethylene) require *ca.* 7–8 kcal mol^{-1}. Consequently, high values should be expected from the quite stiff molecules of PPS, but certainly not as unrealistically high as those predicted for $\alpha = 0.1$.

The ratio of pre-exponential factors, G_0^{III}/G_0^{II} is determined for our MMW PPS to be 7.1×10^3. While there exists[11] a theoretical relationship from which this ratio may be determined as a function of the work of chain folding, it contains many parameters that are not known for PPS, so that no comparison will be made here. However, the above experimental value is well within the (quite broad) range of values that are estimated on the basis of reasonable choices for these various parameters.

Table 3 Values of thermodynamic parameters for MMW PPS*

	$\alpha = 0.1$	$\alpha = 0.3$
σ (erg/cm^2)	5.6	16.9
σ_e (erg/cm^2)		
Rég. II	375	125
Rég. III	389	130
q (kcal mol^{-1} folds)		
Rég. II	26.2	8.7
Rég. III	27.2	9.1

* Using $U^* = 1400$ cal mol^{-1}, $T_m^0 = 315$°C, $T_\infty = 62$°C, $\rho = 1.43$ g cm^{-3} (ref. 55), $\Delta h_f = 80$ J/g (ref. 51), (020) growth substrate, $a_0 = 4.33$ Å, $b_0 = 5.61$ Å (ref. 55)

Régime I → II transition

It is possible to estimate roughly the temperature at which a hypothetical régime I → II transition would occur in PPS, using the relationship[11]

$$\frac{G^{I}}{G^{III}} = \frac{L^{I}}{L^{III}} \tag{6}$$

where L (the substrate length) is equal to the product of the molecular width (a_0) and the number of crystalline stems. The growth rate in régime I must then equal that in régime II at the transition temperature, from which this temperature can be easily located. By assuming[11] that $L^{III} \simeq 3a_0$ and that $0.1\ \mu m \leqslant L^{I} \leqslant 1\ \mu m$, the régime I → II transition would then be expected to occur between 251°C and 263°C depending upon the applicable growth plane and substrate length, as seen in *Table 4*. The shapes of the predicted régime curves as functions of temperature are presented in *Figure 12*, together with our experimental data points. Although we have only one or two data points above the hypothesized régime I → II transitions, these points do not follow the régime I curve, but continue to conform with régime II behaviour. We are not certain of the reasons for this. The relatively small number of stems that a molecule can contribute, and thus the heightened effect of chain ends (particularly in these stiff molecules), may hinder the molecular spreading on the crystal substrate, and therefore retard transition to régime I*. The estimated temperatures of the régime I → II transition may be in slight error because their calculation did not utilize the activation energy for *reptational* transport[37] that should be more appropriate at these high temperatures than the transport term used here; the value of that reptational diffusion term is not known for PPS. The estimate of the substrate length is also in question. From a morphological study[7], we find lamellar widths ~0.1–1 μm in melt-crystallized ultra-thin films, but there is no estimate of their widths in the bulk, nor of the relationship of L to the lamellar width. We do not consider extension of our growth rate data beyond 270°C reliable, because of the inordinately long crystallization times required; we have obtained data up to 275°C, but these are inconclusive due to the alteration of molecular characteristics that accompanies prolonged residence in the melt.

CONCLUSIONS

By crystallizing PPS from both the melt and the quenched glass, we have been able to obtain a most extensive set of growth rate data (ranging from 100°C to 280°C for LMW samples and 115°C to 270°C for MMW samples). These data allowed a reliable search for a régime II → III transition. Such a transition has been found for the MMW sample to be centred at 208°C (although the transition is not sharp, since the specimens are not molecularly monodisperse). For values of the transport parameters $U^* = 1400$ cal mol^{-1} and $T_\infty = T_g - 30$ K (which are close to those from many other polymers) the régime III/II slope ratio is only 3.5% higher than predicted[11]. These values of the transport parameters represent an optimal fit; others (including WLF values) either do not allow linearization of the appropriate plots or yield slope ratios that diverge widely from the theoretical value of 2. Our kinetic analysis has yielded reasonable estimates of lateral- and fold-surface free energies and of the work of chain folding. A régime I → II transition, although predicted to occur at the high-temperature end of our growth-rate data, was not observed. No régime transitions have been found for the LMW specimen for reasons probably associated with the disordering effects of relatively profuse chain ends. As a result, régime III kinetics are followed at low temperatures in this material, with only a gradual approach to régime II at high temperatures.

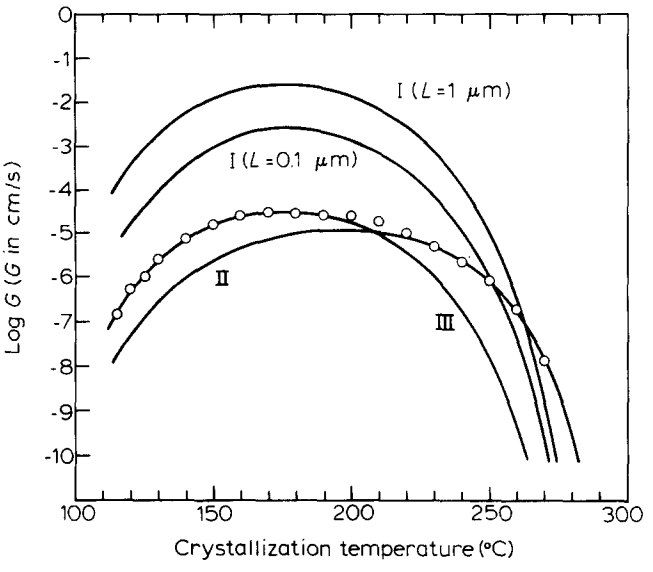

Figure 12 Calculated régime curves superimposed upon the experimental growth rate data for MMW PPS using $U^* = 1400$ cal mol^{-1}, $T_\infty = T_g - 30$ K, $T_m^0 = 315$°C, $T_g = 92$°C. The curves for régime I are based on (020) growth planes

Table 4 Calculated temperatures for hypothetical régime I → II transitions

Growth plane	a_0 (Å)	T for $G_I = G_{II}$ $L = 1\ \mu m$	T for $G_I = G_{II}$ $L = 0.1\ \mu m$
(020)	4.33	263°C	252°C
(110)	5.16	262°C	251°C

* Chain stiffness appears indeed to be the major reason for the lack of a régime I → II transition in PPS, based upon the recent work by J. D. Hoffman on the influence of 'omega'-type defects on effective substrate length (*Polymer*, in press)

ACKNOWLEDGEMENTS

We are grateful to Professor J. D. Hoffman for helpful discussions and for use of a manuscript prior to publication; to Dr T. W. Johnson of Phillips Petroleum Co. for donation of the medium M.wt. PPS sample and for molecular-weight estimates; and to our colleagues H. E. Bair for T_g determinations, R. E. Cais for use of the d.s.c., and H. D. Keith for a very helpful critical review of the manuscript.

REFERENCES

1 Endean, M. H. in '3rd International Conference on Plastics in Telecommunications', Plastics Institute, London, 1983, Ch. 3
2 Boeke, P. J. and DeCallatay, G. ibid., Ch. 4
3 Kelleher, P. G. and Hubbauer, P. '36th ANTEC, Society of Plastics Engineers', 1978, 340

4 Clarke, T. C., Kanazawa, K. K., Lee, V. Y., Rabolt, J. F., Reynolds, J. R. and Street, G. B. *J. Polym. Sci., Polym. Phys. Edn.* 1982, **20**, 117
5 Frommer, J. E., Elsenbaumer, R. L., Eckhardt, H. and Chance, R. R. *J. Polym. Sci., Polym. Lett. Edn.* 1983, **21**, 39
6 Padden, F. J., Jr., Lovinger, A. J. and Davis, D. D. (manuscript in preparation)
7 Lovinger, A. J., Padden, F. J., Jr. and Davis, D. D. *Macromolecules* (to be submitted)
8 Lovinger, A. J. and Davis, D. D. (manuscript in preparation)
9 Hoffman, J. D., Davis, G. T. and Lauritzen, J. I., Jr. in 'Treatise on Solid-State Chemistry', Ed. N. B. Hannay, Plenum Press, New York, 1976, Vol. 3, Ch. 7
10 Lauritzen, J. I., Jr. and Hoffman, J. D. *J. Appl. Phys.* 1973, **44**, 4340
11 Hoffman, J. D. *Polymer* 1983, **24**, 3
12 Martinez-Salazar, J., Barham, P. J. and Keller, A. *J. Polym. Sci., Polym. Phys. Edn.* 1984, **22**, 1085
13 Clark, E. J. and Hoffman, J. D. *Macromolecules* 1984, **17**, 878
14 Pelzbauer, Z. and Galeski, A. *J. Polym. Sci. C* 1972, **38**, 23
15 Dalal, E. N. and Phillips, P. J. *J. Polym. Sci., Polym. Lett. Edn.* 1984, **22**, 7
16 Suzuki, T. and Kovacs, A. J. *Polym. J.* 1970, **1**, 82
17 Keith, H. D. and Padden, F. J., Jr. *J. Appl. Phys.* 1964, **35**, 1286
18 Boon, J., Challa, G. and van Krevelen, D. W. *J. Polym. Sci. A-2* 1968, **6**, 1791
19 Magill, J. H. *Polymer* 1962, **3**, 655
20 Magill, J. H. *Polymer* 1965, **6**, 367
21 Magill, J. H. *J. Polym. Sci. A-2* 1967, **5**, 89
22 Magill, J. H. *J. Polym. Sci. A-2* 1969, **7**, 1187
23 Miller, R. L. in 'Flow-Induced Crystallization', Ed. R. L. Miller, Gordon and Breach, 1979, pp. 31–55
24 Kovacs, A. J. and Gonthier, A. *Kolloid Z.-Z. Polym.* 1972, **250**, 530
25 Kovacs, A. J., Gonthier, A. and Straupe, C. *J. Polym. Sci., Polym. Symp. Edn.* 1975, **50**, 283
26 Ferry, J. D. 'Viscoelastic Properties of Polymers', 3rd ed., Wiley, New York, 1980
27 Williams, M. L., Landel, R. F. and Ferry, J. D. *J. Am. Chem. Soc.* 1955, **77**, 3701
28 Magill, J. H. *J. Polym. Sci. A* 1965, **3**, 1195
29 Burnett, B. B. and McDevit, W. F. *J. Appl. Phys.* 1957, **28**, 1101
30 Gilbert, M. and Hybart, F. J. *Polymer* 1972, **13**, 327
31 Powers, J., Hoffman, J. D., Weeks, J. J. and Quinn, F. A., Jr. *J. Res. Natl. Bur. Stand.* 1965, **69A**, 335
32 von Falkai, B. and Rellensmann, W. *Makromol. Chem.* 1964, **75**, 112
33 Hoffman, J. D. and Weeks, J. J. *J. Chem. Phys.* 1962, **37**, 1723
34 Flory, P. J. and McIntyre, A. D. *J. Polym. Sci.* 1955, **18**, 592
35 Sharples, A. and Swinton, F. L. *Polymer* 1963, **4**, 119
36 Hoffman, J. D., Frolen, L. J., Ross, G. S. and Lauritzen, J. I., Jr. *J. Res. Natl. Bur. Stand.* 1975, **79A**, 671
37 Hoffman, J. D. *Polymer* 1982, **23**, 656
38 Ueberreiter, K. and Steiner, K. *Makromol. Chem.* 1966, **91**, 175
39 van Antwerpen, F. and van Krevelen, D. W. *J. Polym. Sci., Polym. Phys. Edn.* 1972, **10**, 2423
40 Edwards, B. C. *J. Polym. Sci., Polym. Phys. Edn.* 1975, **13**, 1387
41 Lovering, E. G. *J. Polym. Sci. C* 1970, **30**, 329
42 Vasanthakumari, R. and Pennings, A. J. *Polymer* 1983, **24**, 175
43 Magill, J. H. *Makromol. Chem.* 1965, **86**, 283
44 von Falkai, B. and Stuart, H. A. *Kolloid Z.* 1959, **162**, 138
45 Binsbergen, F. L. and deLange, B. G. M. *Polymer* 1970, **11**, 309
46 Goldfarb, L. *Makromol. Chem.* 1978, **179**, 2297
47 Miller, R. L. and Seeley, E. G. *J. Polym. Sci., Polym. Phys. Edn.* 1982, **20**, 2297
48 Welch, G. J. and Miller, R. L. *J. Polym. Sci., Polym. Phys. Edn.* 1976, **14**, 1683
49 Lovinger, A. J. *J. Polym. Sci., Polym. Phys. Edn.* 1980, **18**, 793
50 Johnson, T. W. (private communication)
51 Brady, D. G. *J. Appl. Polym. Sci.* 1976, **20**, 2541
52 Edmonds, J. T. and Hill, H. W., Jr. U.S. Pat. 3,354,129 (November 1967)
53 Hawkins, R. T. *Macromolecules* 1976, **9**, 189
54 Sergeyev, V. A., Shitikov, V. K., Nedelkin, V. I., Askadskii, A. A., Bychko, K. A., Slonimskii, G. L. and Korshak, V. V. *Polym. Sci. U.S.S.R.* 1977, **19**, 1494
55 Tabor, B. J., Magré, E. P. and Boon, J. *Eur. Polym. J.* 1971, **7**, 1127
56 Hoffman, J. D. and Weeks, J. J. *J. Res. Natl. Bur. Stand.* 1962, **66**, 13
57 Thomas, D. G. and Stavely, L. A. K. *J. Chem. Soc.* 1952, 4569